ELSEVIER

Composite Structures 56 (2002) 25–34

COMPOSITE STRUCTURES

www.elsevier.com/locate/compstruct

Hygrothermal effects on the structural behaviour of thick composite laminates using higher-order theory

B.P. Patel, M. Ganapathi *, D.P. Makhecha

Institute of Armament Technology, Girinagar, Pune 411 025, India

Abstract

Here, static and dynamic characteristics of thick composite laminates exposed to hygrothermal environment are studied using a realistic higher-order theory developed recently. The formulation accounts for the nonlinear variation of the in-plane and transverse displacements through the thickness, and abrupt discontinuity in slope of the in-plane displacements at any interface. The analysis is carried out employing a C^0 QUAD-8 isoparametric higher-order finite element. It is shown that the shear deformation theory without accounting for the thickness-stretching effect and slope discontinuity in the in-plane displacements may not be adequate for the analysis of fairly thick composite laminates exposed to hygrothermal loading. The significance of retaining various higher-order terms in the present model, in evaluating the deflection, buckling and natural frequency for composite laminates at different moisture concentration and temperature, is brought out through parametric study.

Keywords: Laminates; Moisture; Static; Vibration; Buckling; Higher-order; Finite element

1. Introduction

The increased utilization of laminated anisotropic composite structural elements into the construction of aeronautical and aerospace vehicles, as well as civil and mechanical structures are mainly due to the combination features of high modulus, high strength, low weight, and durability, etc. However, the analysis of such structures is a complex task, compared with conventional single layer metallic structures, because of the exhibition of coupling among membrane, torsion and bending strains; weak transverse shear rigidities; and discontinuity of the mechanical characteristics along the thickness of the laminates. For these reasons, in recent years, there is a great deal of research interest for accurately modeling and simulating the characteristics of composite structures through different higher-order displacement functions for two-dimensional theories as they lead to less expensive models compared to three-dimensional one. In this context, the applications of analytical/numerical methods based on various 2D higher-order theories for static and dynamic analyses of rectangular laminates have recently attracted the attention of several investigators/researchers.

Various structural theories proposed for evaluating the characteristics of composite laminates under different loading situations have been reviewed and assessed by Noor and Burt [1,2], Tauchert [3], Kapania and Raciti [4], Reddy [5], and more recently by Mallikarjuna and Kant [6]. The important studies considering hygrothermal effects include the work of [7–12]. It may be concluded from the literature that the analysis of composite plates subjected to hygrothermal environment is generally based on the classical lamination theory, and first-order shear deformation theory. For accurate prediction, the higher-order displacement fields yielding quadratic variation of transverse shear strains have been introduced by many researchers [13–20] for the analysis of laminates subjected to mechanical load. But the application of higher-order theories for the study of thick multi-layered laminates [2,6] under hygrothermal–mechanical load seems to be scarce in the literature.

Three-dimensional elasticity analysis carried out by Bhaskar et al. [21] for thick laminates subjected to thermal loads reveals the non-linear variation of in-plane displacements through the thickness and abrupt discontinuity in slope at any interface, and thickness-stretch/contraction effects in the transverse displacement. Although higher-order theories based on discrete

* Corresponding author. Tel.: +91-020-4389550; fax: +91-020-4389509.

E-mail addresses: mganapathi@hotmail.com, gana@iat.ernet.in (M. Ganapathi).

0263-8223/02/$ - see front matter
PII: S0263-8223(01)00182-9

layer approach [22–26] account for slope discontinuity at the interfaces, the number of unknowns to be solved increases with the increase in the number of layers. Recently, Ali et al. [27] have proposed a new higher-order plate theory based on global approximation approach for the static analysis of multi-layered symmetric composite laminates incorporating realistic through the thickness approximations of the in-plane and transverse displacements. This formulation has proved to give very accurate results for the static analysis of symmetric cross-ply laminates, and this excellent performance of the theory for thick laminates motivated the present extension of the formulation for studying the hygrothermal effects on the laminates through finite element procedure.

Here, a C^0 eight-noded quadrilateral serendipity plate element developed with thirteen degrees of freedom per node is used for the static and dynamic characteristics of thick composite laminates. The formulation is general in the sense that it is applicable for the analysis of plates subjected to temperature/moisture variation through the volume of the laminates. The analysis also accounts for reduced lamina material properties at the elevated moisture concentration and temperature. The effects of various terms in the higher-order displacement model in predicting the responses such as deflection, buckling load and natural frequencies of laminates subjected to the exposure of hygrothermal environment are discussed.

2. Formulation

A composite plate with arbitrary lamination is considered with the co-ordinates x, y along the in-plane directions and z along the thickness direction. The in-plane displacements u^k and v^k, and the transverse displacement w^k for the kth layer are assumed as

$$\begin{aligned} u^k(x,y,z,t) &= u_0(x,y,t) + z\theta_x(x,y,t) + z^2\beta_x(x,y,t) \\ &\quad + z^3\phi_x(x,y,t) + S^k\psi_x(x,y,t), \\ v^k(x,y,z,t) &= v_0(x,y,t) + z\theta_y(x,y,t) + z^2\beta_y(x,y,t) \\ &\quad + z^3\phi_y(x,y,t) + S^k\psi_y(x,y,t), \\ w^k(x,y,z,t) &= w_0(x,y,t) + zw_1(x,y,t) + z^2\Gamma(x,y,t). \end{aligned} \tag{1}$$

The terms with even power in z in the in-plane displacements and those odd in z occurring in the expansion for w^k correspond to stretching problems. But, the terms with odd in z in the in-plane displacements and those even in z in the expression for w^k represent the flexure problems. u_0, v_0, w_0 are the displacements of a generic point on the reference surface; θ_x, θ_y are the rotations of normal to the reference surface about the y and x axes, respectively; w_1, β_x, β_y, Γ, ϕ_x, ϕ_y are the higher-order terms in Taylor's series expansions, defined at the reference surface. ψ_x and ψ_y are generalized variables associated with the zig-zag function, S^k. The zig-zag function, S^k, as given in [28], is defined by

$$S^k = 2(-1)^k z_k/h_k, \tag{2}$$

where z_k is the local transverse coordinate with its origin at the centre of the kth layer and h_k is the corresponding layer thickness. Thus, the zig-zag function is piecewise linear with values of -1 and 1 alternately at the different interfaces. The 'zig-zag' function, as defined above, takes care of inclusion of the slope discontinuity of u and v at the interfaces of the laminate as observed in exact three-dimensional elasticity solutions of thick laminated composite structures. The use of such function is more economical than a discrete layer approach of approximating the displacement variations over the thickness of each layer separately. Although both these approaches account for slope discontinuity at the interfaces, in the discrete layer approach the number of unknowns increases with the increase in the number of layers, whereas it remains constant in the present approach.

The strains in terms of mid-plane deformation, rotations of normal, and higher-order terms associated with displacements for kth layer are

$$\{\varepsilon\} = \begin{Bmatrix} \varepsilon_{\mathrm{bm}} \\ \varepsilon_{\mathrm{s}} \end{Bmatrix} - \{\bar{\varepsilon}_0\} + \{\varepsilon_{\mathrm{NL}}\}. \tag{3}$$

The vector $\{\varepsilon_{\mathrm{bm}}\}$ includes the bending and membrane terms of the strain components and vector $\{\varepsilon_{\mathrm{s}}\}$ contains the transverse shear strain terms. These strain vectors can be defined as

$$\begin{aligned} \begin{Bmatrix} \varepsilon_{\mathrm{bm}} \\ \varepsilon_{\mathrm{s}} \end{Bmatrix} &= \begin{Bmatrix} \varepsilon_{xx} \\ \varepsilon_{yy} \\ \varepsilon_{zz} \\ \varepsilon_{xy} \\ \gamma_{xz} \\ \gamma_{yz} \end{Bmatrix} = \begin{Bmatrix} u^k_{,x} \\ v^k_{,y} \\ w^k_{,z} \\ u^k_{,y} + v^k_{,x} \\ u^k_{,z} + w^k_{,x} \\ v^k_{,z} + w^k_{,y} \end{Bmatrix} \\ &= [\overline{Z}]\{\,\varepsilon_0 \quad \varepsilon_1 \quad \varepsilon_2 \quad \varepsilon_3 \quad \varepsilon_4 \quad \gamma_0 \quad \gamma_1 \quad \gamma_2 \quad \gamma_3\,\}^{\mathrm{T}}, \end{aligned} \tag{4a}$$

where

$$[\overline{Z}] = \begin{bmatrix} [I_1] & z[I_1] & z^2[I_1] & z^3[I_1] & S^k[I_1] & [O] & [O] & [O] & [O] \\ [O]^{\mathrm{T}} & [O]^{\mathrm{T}} & [O]^{\mathrm{T}} & [O]^{\mathrm{T}} & [O]^{\mathrm{T}} & [I_2] & z[I_2] & z^2[I_2] & S^k_{,z}[I_2] \end{bmatrix}. \tag{4b}$$

$[I_1]$ and $[I_2]$ are identity matrices of size 4×4 and 2×2, respectively, and $[O]$ is null matrix of size 4×2:

$$\{\varepsilon_0\} = \begin{Bmatrix} u_{0,x} \\ v_{0,y} \\ w_1 \\ u_{0,y} + v_{0,x} \end{Bmatrix}, \quad \{\varepsilon_1\} = \begin{Bmatrix} \theta_{x,x} \\ \theta_{y,y} \\ 2\Gamma \\ \theta_{x,y} + \theta_{y,x} \end{Bmatrix},$$

$$\{\varepsilon_2\} = \begin{Bmatrix} \beta_{x,x} \\ \beta_{y,y} \\ 0 \\ \beta_{x,y} + \beta_{y,x} \end{Bmatrix}, \quad \{\varepsilon_3\} = \begin{Bmatrix} \phi_{x,x} \\ \phi_{y,y} \\ 0 \\ \phi_{x,y} + \phi_{y,x} \end{Bmatrix}, \tag{4c}$$

$$\{\varepsilon_4\} = \begin{Bmatrix} \psi_{x,x} \\ \psi_{y,y} \\ 0 \\ \psi_{x,y} + \psi_{y,x} \end{Bmatrix},$$

$$\{\gamma_0\} = \begin{Bmatrix} \theta_x + w_{0,x} \\ \theta_y + w_{0,y} \end{Bmatrix}, \quad \{\gamma_1\} = \begin{Bmatrix} 2\beta_x + w_{1,x} \\ 2\beta_y + w_{1,y} \end{Bmatrix},$$

$$\{\gamma_2\} = \begin{Bmatrix} 3\phi_x + \Gamma_{,x} \\ 3\phi_y + \Gamma_{,y} \end{Bmatrix}, \quad \{\gamma_3\} = \begin{Bmatrix} \psi_x \\ \psi_y \end{Bmatrix}. \tag{4d}$$

The subscript comma denotes the partial derivative with respect to the spatial coordinate succeeding it.

The strain vector $\{\bar{\varepsilon}_0\}$ due to temperature and moisture is represented as

$$\left\{\bar{\varepsilon}_0\right\} = \begin{Bmatrix} \bar{\varepsilon}_{xx} \\ \bar{\varepsilon}_{yy} \\ \bar{\varepsilon}_{zz} \\ \bar{\varepsilon}_{xy} \\ \bar{\varepsilon}_{xz} \\ \bar{\varepsilon}_{yz} \end{Bmatrix} = \Delta T \begin{Bmatrix} \alpha_x \\ \alpha_y \\ \alpha_z \\ \alpha_{xy} \\ 0 \\ 0 \end{Bmatrix} + \Delta C \begin{Bmatrix} \mu_x \\ \mu_y \\ \mu_z \\ \mu_{xy} \\ 0 \\ 0 \end{Bmatrix}, \tag{4e}$$

where ΔT and ΔC are the rise in temperature and moisture concentration, respectively, and are generally represented as function of x, y, z and time t. α_x, α_y, α_z and α_{xy} are thermal expansion coefficients in the plate coordinates and can be related to the thermal coefficients (α_1, α_2 and α_3) in the material principal directions. μ_x, μ_y, μ_z and μ_{xy} are moisture expansion coefficients similar to thermal expansion coefficients in the plate coordinates.

The nonlinear strain vector $\{\varepsilon_{\mathrm{NL}}\}$ is defined as

$$\{\varepsilon_{\mathrm{NL}}\} = \begin{Bmatrix} \varepsilon_{xx}^{\mathrm{NL}} \\ \varepsilon_{yy}^{\mathrm{NL}} \\ \varepsilon_{zz}^{\mathrm{NL}} \\ \varepsilon_{xy}^{\mathrm{NL}} \\ \varepsilon_{xz}^{\mathrm{NL}} \\ \varepsilon_{yz}^{\mathrm{NL}} \end{Bmatrix} = \begin{Bmatrix} (1/2)(u_{,x}^{k2} + v_{,x}^{k2} + w_{,x}^{k2}) \\ (1/2)(u_{,y}^{k2} + v_{,y}^{k2} + w_{,y}^{k2}) \\ (1/2)(u_{,z}^{k2} + v_{,z}^{k2} + w_{,z}^{k2}) \\ u_{,x}^{k}u_{,y}^{k} + v_{,x}^{k}v_{,y}^{k} + w_{,x}^{k}w_{,y}^{k} \\ u_{,x}^{k}u_{,z}^{k} + v_{,x}^{k}v_{,z}^{k} + w_{,x}^{k}w_{,z}^{k} \\ u_{,y}^{k}u_{,z}^{k} + v_{,y}^{k}v_{,z}^{k} + w_{,y}^{k}w_{,z}^{k} \end{Bmatrix}. \tag{4f}$$

The constitutive relations for an arbitrary layer k, in the laminate (x, y, z) coordinate system can be expressed as

$$\{\sigma\} = \{\, \sigma_{xx} \quad \sigma_{yy} \quad \sigma_{zz} \quad \tau_{xy} \quad \tau_{xz} \quad \tau_{yz} \,\}^{\mathrm{T}}$$
$$= [\overline{Q}_k]\left\{ \begin{Bmatrix} \varepsilon_{\mathrm{bm}} \\ \varepsilon_{\mathrm{s}} \end{Bmatrix} - \{\bar{\varepsilon}_0\} + \{\varepsilon_{\mathrm{NL}}\} \right\}, \tag{5}$$

where the terms of $[\overline{Q}_k]$ matrix of kth ply are referred to the laminate axes and can be obtained from the $[Q_k]$ corresponding to the fibre directions with the appropriate transformation, as outlined in the literature [29]. $\{\sigma\}, \{\varepsilon\}, \{\bar{\varepsilon}_0\}, \{\varepsilon_{\mathrm{NL}}\}$ are stress, total strain, strain vectors due to rise in temperature and moisture, and nonlinear strain. The superscript T refers the transpose of a matrix/vector.

The governing equations are obtained by applying Lagrangian equations of motion given by

$$\frac{\mathrm{d}}{\mathrm{d}t}[\partial(T - U_{\mathrm{T}})/\partial\dot{\delta}_i] - [\partial(T - U_{\mathrm{T}})/\partial\delta_i] = 0, \quad i = 1 \text{ to } n, \tag{6}$$

where T is the kinetic energy; U_{T} is the total potential energy consisting of strain energy contributions due to the in-plane and transverse stresses, and work done by the externally applied mechanical loads, respectively. $\{\delta\} = \{\delta_1, \delta_2, \ldots, \delta_i, \ldots, \delta_n\}^{\mathrm{T}}$ is the vector of the degree of freedoms/generalized coordinates. A dot over the variables represents the partial derivative with respect to time.

The kinetic energy of the plate is given by

$$T(\delta) = \frac{1}{2}\int\int\left[\sum_{k=1}^{n}\int_{h_k}^{h_{k+1}} \rho_k \left\{ \dot{u}^k \quad \dot{v}^k \quad \dot{w}^k \right\} \times \left\{ \dot{u}^k \quad \dot{v}^k \quad \dot{w}^k \right\}^{\mathrm{T}} \mathrm{d}z\right] \mathrm{d}x\,\mathrm{d}y, \tag{7}$$

where ρ_k is the mass density of the kth layer. h_k, h_{k+1} are the z coordinates of laminate corresponding to the bottom and top surfaces of the kth layer.

Using the kinematics given in Eq. (1), Eq. (7) can be rewritten as

$$T(\delta) = \frac{1}{2}\int\int\left[\sum_{k=1}^{n}\int_{h_k}^{h_{k+1}} \rho_k \{\dot{d}^{\mathrm{e}}\}^{\mathrm{T}}[Z]^{\mathrm{T}}[Z]\left\{\dot{d}^{\mathrm{e}}\right\}\mathrm{d}z\right]\mathrm{d}x\,\mathrm{d}y, \tag{8}$$

where

$$\{\dot{d}^{\mathrm{e}}\}^{\mathrm{T}} = \{\, \dot{u}_0 \quad \dot{v}_0 \quad \dot{w}_0 \quad \dot{\theta}_x \quad \dot{\theta}_y \quad \dot{w}_1 \quad \dot{\beta}_x \quad \dot{\beta}_y \quad \dot{\Gamma} \quad \dot{\phi}_x \quad \dot{\phi}_y \quad \dot{\Psi}_x \quad \dot{\Psi}_y \,\}$$

and

$$[Z] = \begin{bmatrix} 1 & 0 & 0 & z & 0 & 0 & z^2 & 0 & 0 & z^3 & 0 & S^k & 0 \\ 0 & 1 & 0 & 0 & z & 0 & 0 & z^2 & 0 & 0 & z^3 & 0 & S^k \\ 0 & 0 & 1 & 0 & 0 & z & 0 & 0 & z^2 & 0 & 0 & 0 & 0 \end{bmatrix}.$$

The potential energy functional U_1 (due to internal strain and transverse load) is given by

$$U_1(\delta) = \frac{1}{2}\int\int\left[\sum_{k=1}^{n}\int_{h_k}^{h_{k+1}} \{\sigma\}^{\mathrm{T}}\{\varepsilon\}\,\mathrm{d}z\right]\mathrm{d}x\,\mathrm{d}y - \int\int qw\,\mathrm{d}x\,\mathrm{d}y, \tag{9}$$

where q is the distributed force acting on the top surface of the plate.

Substituting the constitutive relation, Eq. (5), in Eq. (9) one can write U_1 as

$$\begin{aligned} U_1(\delta) = \frac{1}{2}\int\int\left[\sum_{k=1}^{n}\int_{h_k}^{h_{k+1}}\left(\{\varepsilon_{bm}\varepsilon_s\}^T[\overline{Q}]\{\varepsilon_{bm}\varepsilon_s\}\right.\right. \\ - 2\{\varepsilon_{bm}\varepsilon_s\}^T[\overline{Q}]\left\{\bar{\varepsilon}_0\right\} + \left\{\bar{\varepsilon}_0\right\}^T[\overline{Q}]\left\{\bar{\varepsilon}_0\right\} \\ - 2\{\varepsilon_{NL}\}^T[\overline{Q}]\left\{\bar{\varepsilon}_0\right\} + \{\varepsilon_{NL}\}^T[\overline{Q}]\{\varepsilon_{NL}\} \\ \left.\left. + 2\{\varepsilon_{bm}\varepsilon_s\}^T[\overline{Q}]\{\varepsilon_{NL}\}\right)dz\right]dx\,dy \\ - \int\int qw\,dx\,dy. \end{aligned} \tag{10}$$

The potential energy due to applied in-plane stress σ^0_{xx} (due to mechanical load in x-direction) is written as

$$U_2(\delta) = \int\int\left[\sum_{k=1}^{n}\int_{h_k}^{h_{k+1}}\varepsilon^{NL}_{xx}\sigma^0_{xx}\,dz\right]dx\,dy. \tag{11}$$

For obtaining the element level governing equations, the kinetic and the total potential energies (T and $U_T = U_1 + U_2$) may be conveniently written as

$$T(\delta^e) = \frac{1}{2}\{\dot{\delta}^e\}^T[M^e]\{\dot{\delta}^e\}, \tag{12}$$

$$\begin{aligned} U_T(\delta^e) = {} & \frac{1}{2}\{\delta^e\}^T[K^e]\{\delta^e\} + \frac{1}{2}\{\delta^e\}^T\left[K^e_R\right]\{\delta^e\} \\ & + \frac{1}{2}\{\delta^e\}^T\left[K^e_G\right]\{\delta^e\} + \frac{1}{2}\{\delta^e\}^T\left[K^e_{NL}\right]\{\delta^e\} \\ & - \{\delta^e\}^T\left\{F^e_T\right\} - \{\delta^e\}^T\left\{F^e_M\right\} \\ & + \frac{1}{2}\int\int\left[\sum_{k=1}^{n}\int_{h_k}^{h_{k+1}}\{\bar{\varepsilon}_0\}^T[\overline{Q}]\{\bar{\varepsilon}_0\}\,dz\right]dx\,dy. \end{aligned} \tag{13}$$

Here, $[K^e]$, $[K^e_{NL}]$ are the elemental linear and nonlinear stiffness matrices; $[K^e_R]$, $[K^e_G]$ are the geometric stiffness matrices due to residual stresses and applied in-plane mechanical loads, respectively; $[M^e]$ be the mass matrix; $\{F^e_T\}$, $\{F^e_M\}$ are the hygrothermal and mechanical load vectors, respectively. Here δ^e is the vector of the elemental degrees of freedoms/generalized coordinates.

Substituting Eqs. (12) and (13) in Eq. (6), one obtains the governing equation for the element as

$$\begin{aligned} & [M^e]\{\ddot{\delta}^e\} + [K^e]\{\delta^e\} + [K^e_{NL}]\{\delta^e\} + [K^e_R]\{\delta^e\} + [K^e_G]\{\delta^e\} \\ & \quad = \{F^e_T\} + \{F^e_M\}. \end{aligned} \tag{14}$$

The coefficients of mass and various stiffness matrices, and the load vectors involved in governing equation (14) can be rewritten as the product of term having thickness co-ordinate z alone and the term containing x and y. In the present study, while performing the integration, terms having thickness co-ordinate z are explicitly integrated whereas the terms containing x and y are evaluated using full integration with 3×3 points Gauss integration rule.

Following the usual finite element assembly procedure, the governing equation of the laminate are obtained as

$$\begin{aligned} & [M]\{\ddot{\delta}\} + [K]\{\delta\} + [K_{NL}]\{\delta\} + [K_R]\{\delta\} + [K_G]\{\delta\} \\ & \quad = \{F_T\} + \{F_M\}. \end{aligned} \tag{15}$$

Here, $[K]$, $[K_{NL}]$ are the global linear and nonlinear stiffness matrices; $[K_R]$, $[K_G]$ are the global geometric stiffness matrices due to residual stresses and applied in-plane mechanical loads, respectively; $[M]$ be the global mass matrix; $\{F_T\}$, $\{F_M\}$ are the global hygrothermal and mechanical load vectors.

For linear static, buckling and free vibration analyses, the governing equations are:

$$\text{Static}: \quad [K]\{\delta\} = \{F_T\} + \{F_M\}, \tag{15a}$$

$$\text{Buckling}: \quad [K]\{\delta\} + [K_R]\{\delta\} - \lambda\left[K^*_G\right]\{\delta\} = \{0\}, \tag{15b}$$

$$\text{Free vibration}: \quad [M]\{\ddot{\delta}\} + [K]\{\delta\} + [K_R]\{\delta\} = \{0\}, \tag{15c}$$

where $[K^*_G]$ is the geometric stiffness matrix due to unit in-plane mechanical load.

The residual stress state developed in the plate very much depends on the lay-up. Hence, to evaluate such stress state, prebuckling displacement field for the assumed hygrothermal–mechanical load is obtained using Eq. (15a). This displacement field is then used to calculate the stresses and in turn, $[K_R]$, $[K_G]$ matrices.

3. Element description

In the present work, a simple, C^0 continuous, eight-noded serendipity quadrilateral shear flexible plate element with 13 degrees of freedom ($u_0, v_0, w_0, \theta_x, \theta_y, w_1, \beta_x, \beta_y, \Gamma, \phi_x, \phi_y, \psi_x$ and ψ_y: 13-DOF) is employed.

The finite element represented as per the kinematics given in Eq. (1) is referred as HSDT13 with cubic variation. Four more alternate discrete models are proposed, to study the influence of higher-order terms in the displacement functions, whose displacement fields are deduced from the original element by deleting the appropriate degrees of freedom (w_1 and $\Gamma = 0$; or $\psi = 0$; or z^2 terms, ψ, w_1 and $\Gamma = 0$; or dropping all the higher-order terms). These alternate models, and the corresponding degrees of freedom are shown in Table 1.

Table 1
Alternate eight-noded finite element models considered for parametric study

Finite element model	Degrees of freedom per node
HSDT13 (present)	$u_0, v_0, w_0, \theta_x, \theta_y, w_1, \beta_x, \beta_y, \Gamma, \phi_x, \phi_y, \psi_x, \psi_y$
HSDT11a	$u_0, v_0, w_0, \theta_x, \theta_y, \beta_x, \beta_y, \phi_x, \phi_y, \psi_x, \psi_y$
HSDT11b	$u_0, v_0, w_0, \theta_x, \theta_y, w_1, \beta_x, \beta_y, \Gamma, \phi_x, \phi_y$
HSDT7	$u_0, v_0, w_0, \theta_x, \theta_y, \phi_x, \phi_y$
FSDT	$u_0, v_0, w_0, \theta_x, \theta_y$

4. Results and discussion

The study, here, has been focussed on the effects of different moisture concentrations/temperature in the plates, in predicting the structural behaviour of composite laminates. Although the formulation presented here is general, the analysis is carried out for cross-ply simply supported composite laminates subjected to uniform distributions of moisture/temperature. Since the higher-order theory, in general, is required for the accurate analysis of thick composite structures, the emphasis in the present work is placed on thick laminates for the numerical study. The influences of various higher-order terms in the displacement field on the results of cross-ply laminates are highlighted considering different thickness ratios and number of layers. The first layer corresponds to the bottom most layer and the ply-angle is measured from x-axis in an anti-clockwise direction. All the layers are of equal thickness.

Based on progressive mesh refinement, an 8×8 grid mesh is found to be adequate to model the full laminates for the present analysis. The reduced lamina material properties at the elevated moisture concentrations and temperature are used in the present analysis and they are given in Table 2. Before proceeding for the detailed study, the formulation developed herein is validated against available closed form/analytical solutions. Table 3 shows the comparison of present solution against the exact solutions of three-dimensional elasticity theory [21], considering the deflections of the laminate subjected to thermal and mechanical loads. For free vibration analysis, the fundamental frequencies obtained by varying the degree of orthotropicity of the layers are given in Table 4 along with three-dimensional elasticity solution [30]. It can be noticed from these tables that the present results are in good agreement with the existing literature. Further,

Table 2
Elastic moduli of graphite/epoxy lamina (a) at different moisture concentration: $G_{13} = G_{12}$, $G_{23} = 0.5G_{12}$, $\nu_{12} = 0.3$, $\beta_1 = 0$ and $\beta_2 = 0.44$; (b) at different temperatures: $G_{13} = G_{12}$, $G_{23} = 0.5G_{12}$, $\nu_{12} = 0.3$, $\alpha_1 = -0.3 \times 10^{-6}$/K and $\alpha_2 = 28.1 \times 10^{-6}$/K

Elastic moduli (GPa)	Moisture concentration, C (%)						
	0.00	0.25	0.50	0.75	1.00	1.25	1.50
E_1	130	130	130	130	130	130	130
E_2	9.5	9.25	9.0	8.75	8.5	8.5	8.5
G_{12}	6.0	6.0	6.0	6.0	6.0	6.0	6.0
	Temperature, T (K)						
	300	325	350	375	400	425	
E_1	130	130	130	130	130	130	
E_2	9.5	8.5	8.0	7.5	7.0	6.75	
G_{12}	6.0	6.0	5.5	5.0	4.75	4.5	

Table 3
Non-dimensional displacement of simply supported three-layered cross-ply square laminates ($E_1/E_2 = 25$, $G_{12}/E_2 = G_{13}/E_2 = 0.5$, $G_{23}/E_2 = 0.2$, $\nu_{12} = \nu_{13} = \nu_{23} = 0.25$, $E_2 = E_3$) due to thermal and mechanical loading for different thickness ratios, $S = a/h$

S	Theory	Thermal loading ($T_0 \sin \pi x/a \sin \pi y/b$)			Mechanical loading ($q_0 \sin \pi x/a \sin \pi y/b$)		
		$\bar{u}(0, b/2, h/2)$	$\bar{v}(a/2, 0, h/2)$	$\bar{w}(a/2, b/2, h/2)$	$\bar{u}(0, b/2, h/2)$	$\bar{v}(a/2, 0, h/2)$	$\bar{w}(a/2, b/2, h/2)$
4	Present	17.83	81.23	42.33	0.959	2.265	2.102
	Elasticity [21]	18.11	81.23	42.69	0.9694	2.281	2.006
10	Present	16.59	31.92	17.37	0.738	1.108	0.753
	Elasticity [21]	16.61	31.95	17.39	0.7351	1.099	0.753
20	Present	16.16	20.34	12.11	0.693	0.795	0.517
	Elasticity [21]	16.17	20.34	12.12	0.6926	0.7944	0.5164
50	Present	16.02	16.72	10.50	0.680	0.697	0.445
	Elasticity [21]	16.02	16.71	10.50	0.6799	0.6967	0.4451

$(\bar{u}, \bar{v}) = (u, v)/(h\alpha_1 T_0 S)$ or $(u, v)(100E_2/q_0 h S^3)$, and $\bar{w} = w/(h\alpha_1 T_0 S^2)$ or $w(100E_2/q_0 h S^4)$.

Table 4
Non-dimensional fundamental frequencies ($\bar{\omega} = \omega\sqrt{\rho h^2/E_2} \times 10$) of simply supported cross-ply square plates with $S = 5$ ($G_{12}/E_1 = 0.6$, $G_{23}/E_2 = 0.5$, $v_{12} = v_{13} = v_{23} = 0.25$, $E_2 = E_3$)

No. of layers, N	Model	E_1/E_2				
		3	10	20	30	40
2	HSDT13	2.4935	2.7886	3.0778	3.2940	3.4638
	Elasticity [30]	2.5031	2.7938	3.0698	3.2705	3.4250
4	HSDT13	2.6029	3.2488	3.7677	4.0841	4.3001
	Elasticity [30]	2.6182	3.2578	3.7622	4.0660	4.2719
6	HSDT13	2.6264	3.3478	3.9219	4.2686	4.5035
	Elasticity [30]	2.6440	3.3657	3.9359	4.2783	4.5091
10	HSDT13	2.6390	3.4018	4.0093	4.3770	4.6279
	Elasticity [30]	2.6583	3.4250	4.0337	4.4011	4.6498

Table 5
Comparison of present results for maximum deflection, critical load and natural frequency of four-layered cross-ply laminates ($a/h = 100$) with closed form solutions

Deflection (mm) Temperature 400 K ($0°/90°/0°/90°$)		Non-dimensional frequency, $\Omega\ (= \omega a^2(\rho/E_2h^2)^{1/2})$ ($0°/90°/90°/0°$)			Non-dimensional critical load, $\overline{N}_{xx}^{cr}\ (= N_{xx}^{cr}/N_{xx}^{*cr})$ ($0°/90°/90°/0°$)		
			Moisture $C = 0.1\%$	Temperature 325 K		Moisture $C = 0.1\%$	Temperature 325 K
Closed form [31]	0.0337	Ritz method [7]	9.4110	8.068	Ritz method [7]	0.6091	0.4477
Present	0.0337	Present	9.3993	8.0531	Present	0.6084	0.4466

N_{xx}^{*cr} is based on FSDT without moisture/temperature.

the maximum deflection of the laminates, critical load and natural frequency of a cross-ply laminate exposed to moisture and temperature are presented in Table 5 along with the closed form [31] and Ritz solutions obtained by extending the approach outlined in [7]. Since the work in [7,31] are based on first order and classical theories, respectively, the present results in Table 5 correspond to FSDT and these compare very well with the available solutions.

The simply supported boundary conditions considered here are

$$v_0 = w_0 = \theta_y = w_1 = \Gamma = \beta_y = \phi_y = \psi_y = 0 \quad \text{at } x = -a/2, a/2,$$
$$u_0 = w_0 = \theta_x = w_1 = \Gamma = \beta_x = \phi_x = \psi_x = 0 \quad \text{at } y = -b/2, b/2.$$

Here a, b refer the length and width of the plate, respectively.

Next, through the present model (HSDT13), the variation of transverse deflection (at $z = 0$ and $h/2$) along the x-axis of two- and eight-layered laminates ($0^0/90^0, [0^0/90^0]_4$) subjected to uniform moisture ($C = 1.5\%$) is evaluated and is given in Figs. 1 and 2 for two values of thickness ratio, $S\ (= a/h = 5$ and 20; $h = 1$ mm). These figures show the effect of higher-order terms pertaining to the present model on the response characteristics, obtained through different finite element models considered in the present study. Since the influence of zig-zag function ψ in the in-plane displacements is insignificant on the transverse displacement for two-layered case (i.e. the results obtained using model HSDT11b almost coincide with that shown for HSDT13), for clarity, the results corresponding to HSDT11b model are not shown in Fig. 1. It is observed from Fig. 1 that the third-order theory, considered here (HSDT7), has negligible effect on the deflection in comparison with those of first-order theory (FSDT). Furthermore, the significance of z^2 term in the in-plane displacement, in addition to less important z^3 term, has been highlighted through FSDT7 and HSDT11a models. However, the predominant contribution on the global response arises from the presence of z^2 term (Γ) in transverse displacement function. It is further viewed that, with the increase in thickness ratio, the effects due to higher-order terms (ψ and z^2 terms in the in-plane displacements) are less appreciable compared to Γ in w expression. The deflection pattern predicted on the top surface of the laminate by HSDT11b and HSDT13 models are apparently different from the rest of the models considered here, irrespective of thickness ratio and number of layers.

With the increase in number of layers, as seen from Fig. 2, the influence of higher-order z^2 term (Γ) in w expression is more compared to first-order model. It is also noticed that, the influence of z^2 terms in the in-plane displacements is predominant on the results and is seen from the HSDT11a and HSDT7 models. It is further evident from Fig. 2 that the zig-zag function ψ in the in-

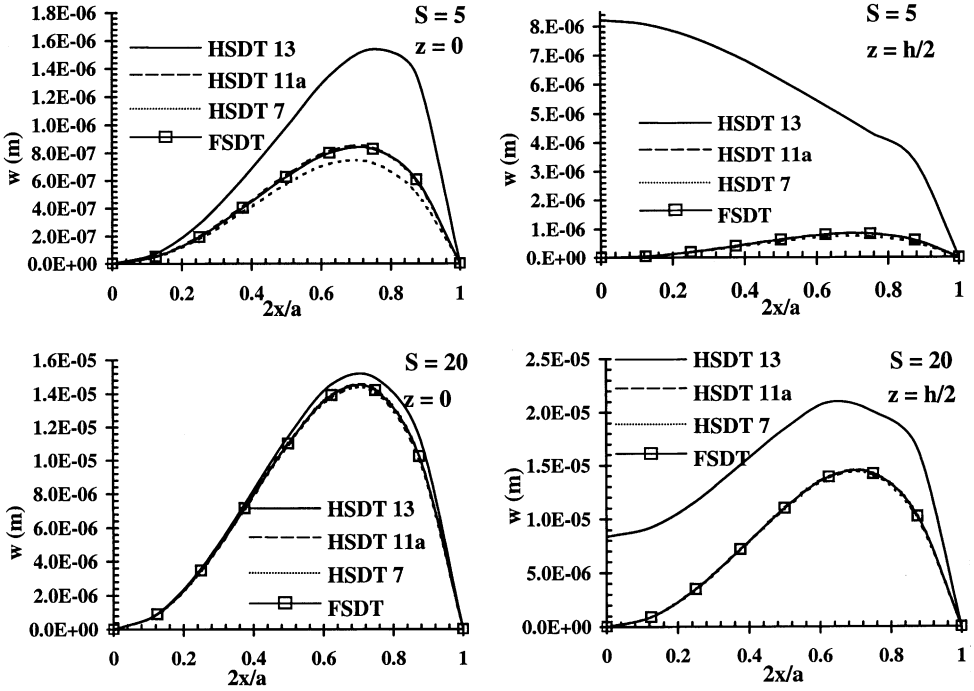

Fig. 1. The variation of transverse displacement due to moisture along the x-axis ($z = 0$ and $h/2$) of two-layered laminates ($S = 5$, 20; $C = 1.5\%$).

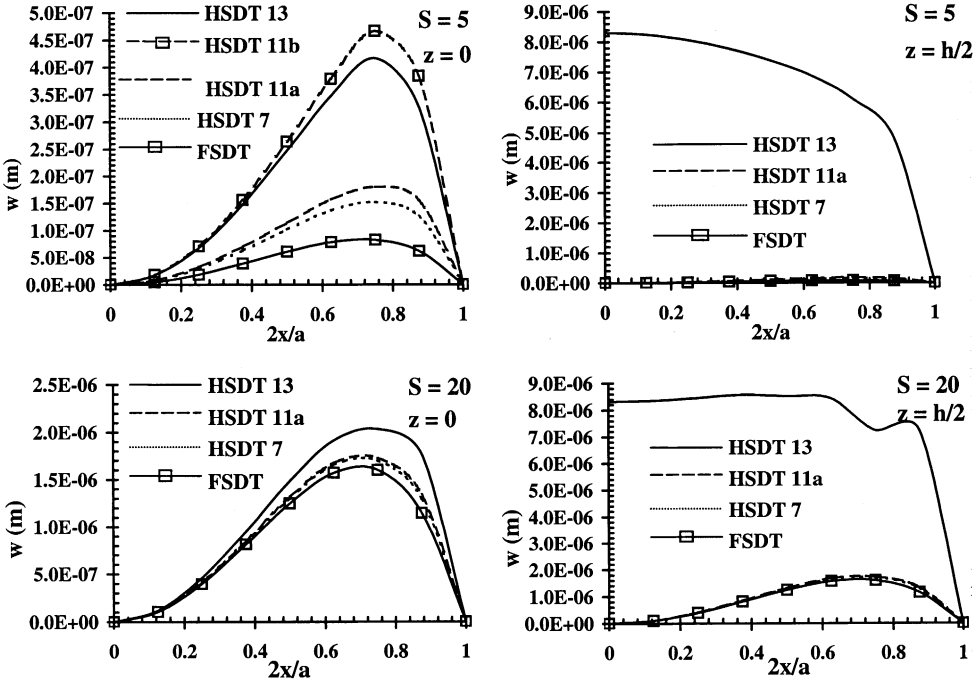

Fig. 2. The variation of transverse displacement due to moisture along the x-axis ($z = 0$ and $h/2$) of eight-layered laminates ($S = 5$, 20; $C = 1.5\%$).

plane displacements has noticeable effects with the increase in layers. It may be opined here that the first-order, and third-order theory of HSDT7 grossly under predicts the transverse displacement. The deflection evaluated away from median surface in the thickness direction is highly dominated by the higher-order z^2 term (Γ) in w function.

Tables 6 and 7 describe the buckling loads ($\overline{N}_{xx}^{\mathrm{cr}} = N_{xx}^{\mathrm{cr}}/N_{xx}^{*cr}; N_{xx}^{*cr}$ is based on FSDT without moisture/temperature) due to applied in-plane force ($N_{xx} = \sigma_{xx}^{0} h$) in the cross-ply composite laminates, initially stressed by the uniform moisture and temperature. The effects of various higher-order terms in the present model on the critical loads are also highlighted. It

Table 6
Effect of moisture concentration on non-dimensional critical load ($\overline{N}_{xx}^{cr}$) of laminates ($S = 5$, 10 and 20)

S	Lay-up	Theory	Moisture concentration (%)						
			0	0.25	0.5	0.75	1	1.25	1.5
5	0°/90°	HSDT13	0.9138	0.8989	0.8718	0.8326	0.7810	0.7176	0.6342
		HSDT11a	0.9122	0.9015	0.8864	0.8672	0.8442	0.8206	0.7909
		HSDT11b	1.0346	1.0248	1.0128	0.9986	0.9815	0.9565	0.9058
		HSDT7	1.0454	1.0363	1.0273	1.0184	1.0097	1.0056	1.0015
		FSDT	1.0000	0.9911	0.9823	0.9735	0.9649	0.9609	0.9567
	$(0°/90°)_4$	HSDT13	0.9281	0.9253	0.9224	0.9193	0.9159	0.9131	0.9097
		HSDT11a	0.9224	0.9192	0.9161	0.9130	0.9099	0.9076	0.9051
		HSDT11b	0.9977	0.9946	0.9894	0.9833	0.9765	0.9702	0.9630
		HSDT7	1.0125	1.0066	1.0008	0.9954	0.9901	0.9861	0.9820
		FSDT	1.0000	0.9964	0.9930	0.9897	0.9854	0.9813	0.9773
10	0°/90°	HSDT13	0.8220	0.7959	0.7490	0.6821	0.5955	0.4858	0.3462
		HSDT11a	0.8218	0.8046	0.7824	0.7556	0.7247	0.6917	0.6518
		HSDT11b	0.9845	0.9602	0.9270	0.8856	0.8363	0.7797	0.7121
		HSDT7	0.9989	0.9781	0.9578	0.9380	0.9189	0.9037	0.8882
		FSDT	1.0000	0.9794	0.9593	0.9396	0.9204	0.9049	0.8890
	$(0°/90°)_4$	HSDT13	0.9763	0.9636	0.9496	0.9348	0.9192	0.9028	0.8847
		HSDT11a	0.9746	0.9623	0.9501	0.9382	0.9266	0.9160	0.9050
		HSDT11b	0.9953	0.9824	0.9684	0.9534	0.9377	0.9213	0.9032
		HSDT7	1.0010	0.9872	0.9740	0.9615	0.9496	0.9389	0.9282
		FSDT	1.0000	0.9863	0.9731	0.9606	0.9487	0.9380	0.9273
20	0°/90°	HSDT13	0.8977	0.8126	0.6624	0.4445	0.1479	–	–
		HSDT11a	0.8972	0.8452	0.7865	0.7219	0.6518	0.5720	0.4801
		HSDT11b	0.9925	0.9242	0.8440	0.7524	0.6499	0.5304	0.3926
		HSDT7	0.9983	0.9389	0.8818	0.8273	0.7752	0.7241	0.6726
		FSDT	1.0000	0.9408	0.8838	0.8291	0.7769	0.7253	0.6731
	$(0°/90°)_4$	HSDT13	0.9923	0.9469	0.8994	0.8501	0.7994	0.7428	0.6817
		HSDT11a	0.9918	0.9513	0.9124	0.8753	0.8399	0.8035	0.7667
		HSDT11b	0.9980	0.9525	0.9050	0.8558	0.8053	0.7488	0.6880
		HSDT7	1.0003	0.9574	0.9167	0.8782	0.8419	0.8047	0.7675
		FSDT	1.0000	0.9572	0.9165	0.8780	0.8417	0.8045	0.7673

Table 7
Effect of temperature on non-dimensional critical load ($\overline{N}_{xx}^{cr}$) of eight-layered laminates ($S = 5$ and 20)

S	Theory	Temperature (K)					
		300	325	350	375	400	425
5	HSDT13	0.8714	0.8526	0.7850	0.7174	0.6790	0.6451
	HSDT11a	0.9235	0.9186	0.8586	0.7970	0.7643	0.7320
	HSDT11b	0.8723	0.8535	0.7857	0.7181	0.6796	0.6457
	HSDT7	1.0153	1.0070	0.9464	0.8805	0.8456	0.8108
	FSDT	1.0000	0.9954	0.9313	0.8650	0.8300	0.7950
20	HSDT13	0.9909	0.9630	0.9271	0.8932	0.8699	0.8481
	HSDT11a	0.9918	0.9627	0.9256	0.8906	0.8661	0.8432
	HSDT11b	0.9967	0.9686	0.9329	0.8994	0.8762	0.8547
	HSDT7	1.0003	0.9699	0.9319	0.8963	0.8711	0.8474
	FSDT	1.0000	0.9696	0.9317	0.8961	0.8709	0.8472

is seen from these tables that the contribution of the zig-zag function ψ in the in-plane displacements is significant on the buckling load in comparison with that of Γ in w function, HSDT11b. It is further observed from these Tables that the critical loads predicted by the HSDT7 model are higher than all other models including FSDT one, irrespective of initial stress due moisture and temperature. It can be viewed from Table 5 that the variation of the results for eight-layered case obtained by different models is qualitatively similar to that of two-layered one. It also shows that the effects of increase in thickness ratio and initial stresses due to moisture and

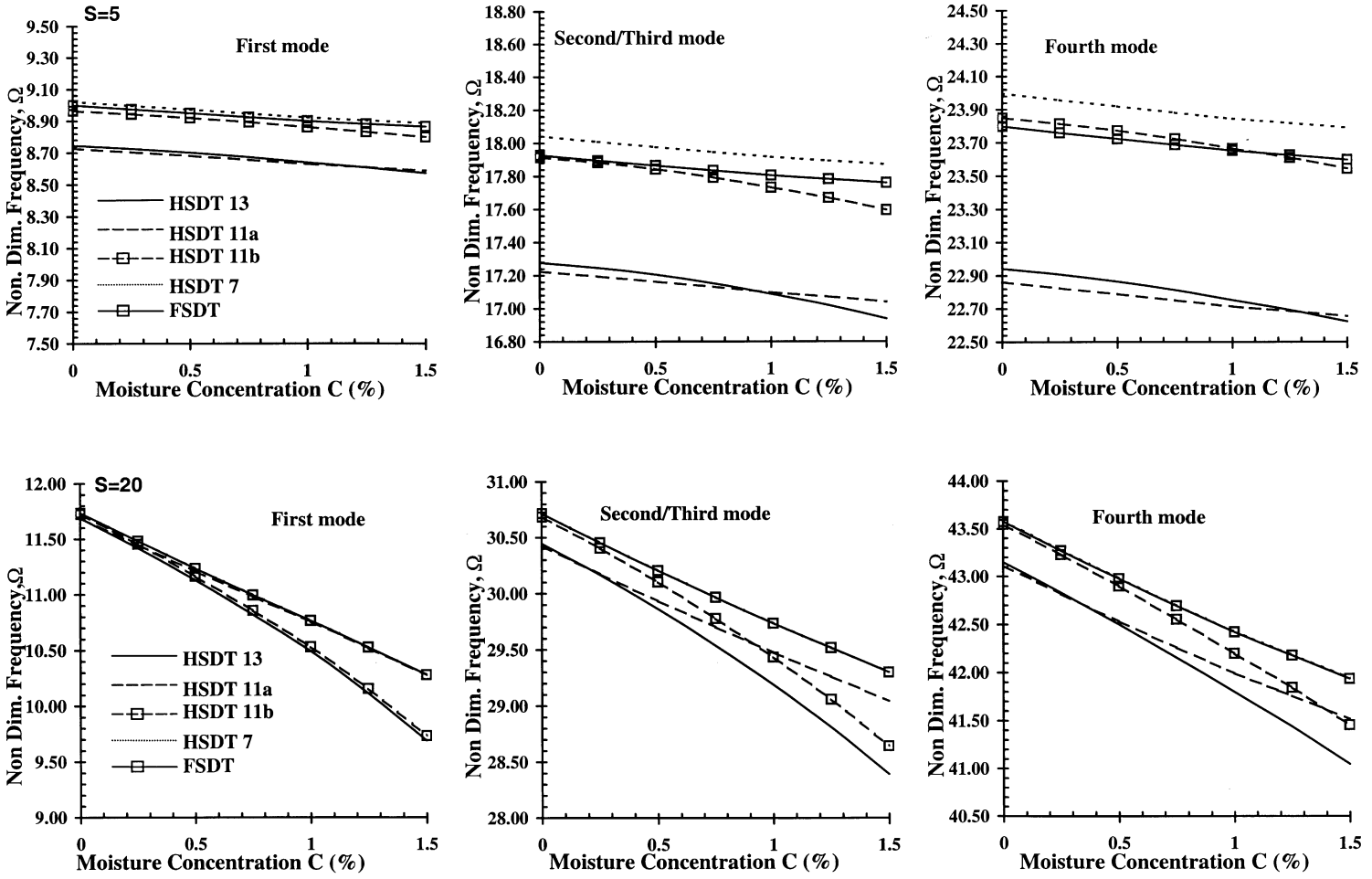

Fig. 3. The variation of natural frequencies ($\Omega = \omega a^2(\rho/E_2h^2)^{1/2}$) of eight-layered laminates with moisture ($S = 5, 20$).

temperature are to reduce the significance of the presence of higher-order terms in the model as expected.

Finally, the influence of moisture on non-dimensional natural frequencies, Ω $(= \omega a^2(\rho/E_2h^2)^{1/2}; \omega$ is the natural frequency) is depicted in Fig. 3 considering different higher-order models. For thick laminate, the inclusion of the zig-zag function ψ in the in-plane displacements is important as seen in the case of buckling study and its effect to the larger extent depends on the moisture concentration. It is also noticed that, with the increase in moisture concentration, the presence of Γ in w function (HSDT11b) gains importance in predicting the frequencies. Furthermore, it is seen that the differences in the results predicted by the models HSDT11b, HSDT7 and FSDT in comparing with those of HSDT13 and HSDT11a increase with mode numbers. The model HSDT7, in general, overpredicts the results. With increase in thickness ratio, incorporation of Γ in w (HSDT11b) is also essential with the increase in moisture concentration.

5. Conclusions

Using an eight-noded C^0 quadrilateral plate element based on realistic theory, the effectiveness of the present formulation over the first- and other higher-order theories for static and dynamic analyses of thick laminates subjected to moisture and temperature has been demonstrated. The inclusion of thickness stretching terms in the transverse displacement field and slope discontinuity in thickness direction for in-plane have pronounced effects on the results and they depend on the type of analysis to be carried out in predicting the accurate response characteristics of composite laminate. For hygrothermal environment, the present formulation (HSDT13) will be more accurate compared to other available models.

References

[1] Noor AK, Burton WS. Assessment of shear deformation theories for multilayered composite plates. ASME Appl Mech Rev 1989;42:1–13.
[2] Noor AK, Burton WS. Computational models for high temperature multilayered plates and shells. ASME Appl Mech Rev 1992;45:419–46.
[3] Tauchert TR. Thermally induced flexure, buckling, and vibration of plates. ASME Appl Mech Rev 1991;44:347–60.
[4] Kapania RK, Raciti S. Recent advances in analysis of laminated beams and plates: Part I: Shear effects and buckling. AIAA J 1989;27:923–34.
[5] Reddy JN. A review of refined theories of composite laminates. Shock Vibr Dig 1990;22:3–17.
[6] Mallikarjuna, Kant T. A critical review and some results of recently developed refined theories of fibre reinforced laminated composites and sandwiches. Compos Struct 1993;23:293–312.
[7] Whitney JM, Ashton JE. Effect of environment on the elastic response of layered composite plates. AIAA 1971;9:1708–13.
[8] Pipes RB, Vinson JR, Chou TW. On the hygrothermal response of laminated composite systems. J Compos Mater 1976;10:129–48.
[9] Snead JM, Papazotto AN. Moisture and temperature effects on the instability of cylindrical composite panel. J Aircraft 1983;20:773–83.
[10] Lee SY, Yen WJ. Hygrothermal effects on the stability of a cylindrical composite shell panel. Comput Struct 1989;33:551–9.
[11] Sai Ram KS, Sinha PK. Hygrothermal effects on the bending characteristics of laminated composite plates. Comput Struct 1991;40:1009–15.
[12] Lee SY, Chou CJ, Jang JL, Lin JS. Hygrothermal effects on the linear and nonlinear analysis of symmetric angle-ply laminated plates, stability of a cylindrical composite shell panel. Compos Struct 1992;21:41–8.
[13] Lo KH, Christensen RM, Wu EM. A higher-order theory of plate deformation. Part 2: Laminated plates. ASME J Appl Mech 1977;44:669–76.
[14] Reddy JN. A simple higher-order theory for laminated composite plates. ASME J Appl Mech 1984;45:745–52.
[15] Phan ND, Reddy JN. Analysis of laminated composite plates using a higher-order shear deformation theory. Int J Numer Meth Eng 1985;21:2201–19.
[16] Kant T, Mallikarjuna. A higher-order theory for free vibration of unsymmetrically laminated composite and sandwich plates – finite element evaluations. Comput Struct 1989;32:1125–32.
[17] Shu X, Sun L. An improved simple higher order theory for a laminated composite plates. Comput Struct 1994;50:231–6.
[18] Shi G, Lam KY, Tay TE. On efficient finite element modelling of composite beams and plates using higher order theories and an accurate composite beam element. Compos Struct 1998;41:159–65.
[19] Franco Correia VM, Mota Soares CM, Mota Soares CA. Higher order models on the eigenfrequency analysis and optimal design of laminated composite structures. Compos Struct 1998;39:237–53.
[20] Khdeir AA, Reddy JN. Free vibrations of laminated composite plates using second-order shear deformation theory. Comput Struct 1999;71:617–26.
[21] Bhaskar K, Varadan TK, Ali JSM. Thermoelastic solutions for orthotropic and anisotropic composite laminates. Composites A 1996;27:415–20.
[22] Reddy JN. A generalization of two-dimensional theories of laminated composite plates. Commun Appl Numer Meth 1987;3:173–80.
[23] Cho KN, Bert CW, Striz AG. Free vibrations of laminated rectangular plates analyzed by higher order individual-layer theory. J Sound Vibr 1991;145:429–42.
[24] Nosier A, Kapania RK, Reddy JN. Free vibration analysis of laminated plates using a layer wise theory. AIAA J 1993;31:2335–46.
[25] Lee KH, Senthilnathan NR, Lim SP, Chow ST. An improved zigzag model for the bending of laminated composites plates. Compos Struct 1990;15:137–48.
[26] Li X, Liu D. Zigzag theory for composite laminates. AIAA J 1995;33:1163–5.
[27] Ali JSM, Bhaskar K, Varadan TK. A new theory for accurate thermal/mechanical flexural analysis of symmetrically laminated plates. Compos Struct 1999;45:227–32.
[28] Murukami H. Laminated composite plate theory with improved in-plane responses. ASME J Appl Mech 1986;53:661–6.
[29] Jones RM. Mechanics of composite materials. New York: McGraw-Hill; 1975.
[30] Noor AK. Free vibrations of multilayered composite plates. AIAA J 1973;11:1038–9.
[31] Wu CH, Tauchert TR. Thermoelastic analysis of laminated plates, 2: Anti-symmetric cross-ply and angle-ply laminates. J Thermal Stresses 1980;3:365–78.